

An 8% Determination of the Hubble Constant from localized Fast Radio Bursts

Q. WU,¹ G. Q. ZHANG,¹ AND F. Y. WANG^{1,2}

¹*School of Astronomy and Space Science, Nanjing University, Nanjing 210093, China*

²*Key Laboratory of Modern Astronomy and Astrophysics (Nanjing University), Ministry of Education, Nanjing 210093, China*

ABSTRACT

The Λ CDM model successfully explains the majority of cosmological observations. However, the Λ CDM model is challenged by Hubble tension, a remarkable difference of Hubble constant H_0 between measurements from local probe and the prediction from Planck cosmic microwave background observations under Λ CDM model. So one urgently needs new distance indicators to test the Hubble tension. Fast radio bursts (FRBs) are millisecond-duration pulses occurring at cosmological distances, which are attractive cosmological probes. However, there is a thorny problem that the dispersion measures (DMs) contributed by host galaxy and the inhomogeneities of intergalactic medium cannot be exactly determined from observations. Previous works assuming fixed values for them bring uncontrolled systematic error in analysis. A reasonable approach is to handle them as probability distributions extracted from cosmological simulations. Here we report a measurement of $H_0 = 64.67^{+5.62}_{-4.66} \text{ km s}^{-1} \text{ Mpc}^{-1}$ using fourteen localized FRBs, with an uncertainty of 8.7% at 68.3 per cent confidence. Thanks to the high event rate of FRBs and localization capability of radio telescopes (i.e., Australian Square Kilometre Array Pathfinder and Very Large Array), future observations of a reasonably sized sample (\sim 100 localized FRBs) will provide a new way of measuring H_0 with a high precision (\sim 2.6%) to test the Hubble tension.

Keywords: cosmology: Hubble constant — Radio bursts

1. INTRODUCTION

The value of Hubble constant (H_0), describing the expansion rate of our universe, is a basic and fascinating issue in cosmology. The measurements of cosmic microwave background (CMB) by Planck Collaboration (Planck Collaboration et al. 2020) are powerful probes to measure cosmological parameters. The distance-redshift relation of specific stars (e.g. Cepheid variables and Type Ia supernovae) can be used constrain Hubble Constant directly (Riess 2020; Riess et al. 2021). Other methods or measurements are also used to measure H_0 , such as Baryon Acoustic Oscillations (BAO), Big Bang Nucleosynthesis (BBN) (Cuceu et al. 2019) and Gravitational Waves (GWs) (Abbott et al. 2017). Great advances in modern observational technology have improved the precision of measuring H_0 .

Corresponding author: F. Y. Wang
 fayinwang@nju.edu.cn

However, a significant difference at least 4σ is reflected in the Hubble constant measured by CMB and Cepheid-calibrated type Ia supernovae (SNe Ia) respectively, known as “Hubble tension” (Freedman 2017; Riess 2020; Di Valentino et al. 2021). New physics or observational bias are two mainstream arguments to alleviate this tension. An independent and robust method of measuring H_0 should be used to test this tension.

Fast radio bursts (FRBs) are short-duration radio pulses with enormous dispersion measures (DMs) (Lorimer et al. 2007; Katz 2018; Petroff et al. 2019; Cordes & Chatterjee 2019; Platts et al. 2019; Xiao et al. 2021). In a short period of more than ten years, a vigorous development has appeared in the observation of FRBs. Up to now, more than 600 FRBs have been observed, including 24 repeating FRBs. Among the 24 repeating FRBs, FRB 121102 and FRB 180916 were found to have periodic activity (Rajwade et al. 2020; Chime/Frb Collaboration et al. 2020). Sub-second periodicity was appeared between the sub-burst of FRB 20191221A reported by CHIME (The CHIME/FRB Collaboration et al. 2021a). There are 15 FRBs with definite host galaxies and redshift measurements, including a neighboring repeating FRB20200120E (Kirsten et al. 2021). The host galaxy association and redshift measurement point out the direction for the study of the origin, radiation mechanism and cosmological application of FRBs.

Dispersion Measure (DM) is defined as the integral of the number density of free electrons along the propagation path, which is positively proportional to cosmological distance. In particular, DM_{IGM} , contributed by the intergalactic medium (IGM), has a close connection with cosmological parameters. Therefore, precise measurements of DM_{IGM} can be used as cosmological probes (Xiao et al. 2021; Bhandari & Flynn 2021), such as “missing” baryons (McQuinn 2014; Macquart et al. 2020), cosmic proper distance (Yu & Wang 2017), dark energy (Zhou et al. 2014; Gao et al. 2014; Walters et al. 2018), Hubble constant (Hagstotz et al. 2021) and reionization history (Zheng et al. 2014; Zhang et al. 2021). Strongly lensed FRBs have been proposed to probe the nature of dark matter (Muñoz et al. 2016; Wang & Wang 2018), and measure Hubble constant (Li et al. 2018). However, how to distinguish them from repeating FRBs is difficult.

In this paper, we propose to measure Hubble constant with 14 localized FRBs through the $DM_{\text{IGM}}-z$ relation. Our paper is organized as the following four sections. In section 2, we present the redshift and DM value of 14 localized FRBs used in our analysis. In section 3, we give an introduction of the distributions of DM_{host} and DM_{IGM} . In section 4, the Monte Carlo Markov Chain (MCMC) analysis is used to constrain the Hubble constant H_0 . The Monte Carlo method is used to simulate FRBs, then the mocked data is used to constrain H_0 . Discussion will be given in section 5.

2. FAST RADIO BURSTS

The DM_{obs} obtained directly from observations can be divided into the following components:

$$DM_{\text{obs}} = DM_{\text{MW}} + DM_{\text{IGM}} + DM_{\text{host}}, \quad (1)$$

where DM_{MW} is contributed by the interstellar medium (ISM) and halo of the Milky Way, DM_{IGM} represents contribution from IGM, DM_{host} is the contribution by FRB host galaxy. It is necessary to consider the value of each term in equation (1) separately. DM_{MW} can be separated into the ISM-contributed $DM_{\text{MW,ISM}}$ and the halo-contributed $DM_{\text{MW,halo}}$. The NE2001 model is used to derive $DM_{\text{MW,ISM}}$ (Cordes & Lazio 2002). This model estimates DM contributions from the galaxy ISM $DM_{\text{MW,ISM}}$ given the orientation of the Galactic-coordinate grids. For the halo-contributed

$\text{DM}_{\text{MW,halo}}$, it has been estimated that the Galactic halo will contribute $50 \sim 80 \text{ pc cm}^{-3}$ from the Sun to 200 kpc (Prochaska & Zheng 2019). Here we assume $\text{DM}_{\text{MW,halo}} = 50 \text{ pc cm}^{-3}$.

For DM_{IGM} , defined as the integral of the number density of free electrons along the sightline in the IGM, contains cosmological information. Central to the analysis is how to get the value of DM_{IGM} . The effect of IGM inhomogeneities will lead to significant sightline-to-sightline scatter around the mean DM_{IGM} (McQuinn 2014). The scatter of DM at $z = 1$ is about 400 pc cm^{-3} from theoretical analysis (McQuinn 2014) and the state-of-the-art cosmological simulations (Jaroszynski 2019; Zhang et al. 2021). Considering a flat universe, the averaged value of DM_{IGM} is (Ioka 2003; Inoue 2004; Deng & Zhang 2014)

$$\langle \text{DM}_{\text{IGM}} \rangle = \frac{3c\Omega_b H_0}{8\pi G m_p} \int_0^{z_{\text{FRB}}} \frac{f_{\text{IGM}}(z) f_e(z) (1+z)}{\sqrt{\Omega_m (1+z)^2 + 1 - \Omega_m}} dz, \quad (2)$$

where m_p is the photon mass. The electron fraction is $f_e(z) = Y_H X_{e,H}(z) + \frac{1}{2} Y_{He} X_{e,He}(z)$, with hydrogen fraction $Y_H = 3/4$ and helium fraction $Y_{He} = 1/4$. Hydrogen and helium are completely ionized at $z < 3$, which implies the ionization fractions of intergalactic hydrogen and helium $X_{e,H} = X_{e,He} = 1$. For a flat ΛCDM model, the density of baryons $\Omega_b h^2 = 0.02235 \pm 0.0049$ is derived by the primordial deuterium abundance combined with a Big Bang nucleosynthesis (BBN) calculation (Cooke et al. 2018), with $h = H_0/100 \text{ km s}^{-1}\text{Mpc}^{-1}$. At present, there is no observation that can give the evolution of the fraction of baryon in the IGM f_{IGM} with redshift. For simplicity but without loss of generality, we assume it as a constant $f_{\text{IGM}} = 0.83$ in this work (Shull et al. 2012).

It is an era of rapid development of radio observation that hundreds of FRBs have been discovered, especially the Canadian Hydrogen Intensity Mapping Experiment (CHIME) has discovered 492 FRBs in a year with its advantage of large field of view (The CHIME/FRB Collaboration et al. 2021b). Currently, only 15 FRBs have been localized including the nearest repeating FRB 200110E (Bhardwaj et al. 2021), which is located in a globular cluster in the direction of the M81 galaxy (Kirsten et al. 2021). The distance of FRB 200110E is only 3.6 Mpc, which is the closest-known extragalactic FRB so far. Correspondingly, the DM value of FRB 200110E is 87.75 pc cm^{-3} . And the intergalactic medium (IGM) contributed $\text{DM}_{\text{IGM}} = 1 \text{ pc cm}^{-3}$ is estimated from the relation of the averaged DM_{IGM} and redshift. Thus the cosmological information carried by FRB 200110E is too seldom to calculate H_0 . Additionally, the effect of peculiar velocity cannot be ignored, which makes it trick to calculate cosmological parameters. Therefore, we excluded FRB 200110E from the localized FRB sample. In general, a sample with a larger amount of data will be more accurate to constrain parameters by reducing the statistical error. Table 1 shows the redshifts, DM_{obs} , $\text{DM}_{\text{MW,ISM}}$, telescopes and references of other 14 localized FRBs. The DM_{IGM} value of FRBs can be estimated using $\text{DM}_{\text{IGM}} = \text{DM}_{\text{obs}} - \text{DM}_{\text{MW,ISM}} - \text{DM}_{\text{MW,halo}} - \text{DM}_{\text{host}}$. Here the value of $\text{DM}_{\text{MW,ISM}}$ is estimated from the NE2001 model (Cordes & Lazio 2002) with the FRB coordinates. We also test our results using the YMW16 model (Yao et al. 2017), and find the effect can be neglected for different free electron distribution models. The value $\text{DM}_{\text{MW,halo}} = 50 \text{ pc cm}^{-3}$ is assumed. The DM_{host} is adopted as the median value derived from the IllustrisTNG simulation (Zhang et al. 2020). Therefore, DM_{IGM} can be estimated by subtracting the above terms and the $\text{DM}_{\text{IGM}}-z$ relation of these FRBs is shown in Figure 1. The estimated DM_{IGM} of 14 localized FRBs are shown as points. The red dotted line is the averaged value of DM_{IGM} from equation (2). The blue solid line is the DM_{IGM} derived from the IllustrisTNG simulation with 95% confidence region (blue shaded area) (Zhang et al. 2021).

Table 1. Properties of localized FRBs

4	Name	Redshift	DM _{obs} (pc cm ⁻³)	DM _{MW,ISM} (pc cm ⁻³)	Telescope	Reference
	FRB 121102	0.19273	557	188.0	Arecibo	Chatterjee et al. (2017)
	FRB 180916	0.0337	348.8	200.0	CHIME	Marcote et al. (2020)
	FRB 180924	0.3214	361.42	40.5	ASKAP	Bannister et al. (2019)
	FRB 181112	0.4755	589.27	102.0	ASKAP	Prochaska et al. (2019)
	FRB 190102	0.291	363.6	57.3	ASKAP	Bhandari et al. (2020)
	FRB 190523	0.66	760.8	37.0	DSA-10	Ravi et al. (2019); Heintz et al. (2020)
	FRB 190608	0.1178	338.7	37.2	ASKAP	Chittidi et al. (2020)
	FRB 190611	0.378	321.4	57.8	ASKAP	Heintz et al. (2020)
	FRB 190614	0.6	959.2	83.5	VLA	Law et al. (2020)
	FRB 190711	0.522	593.1	56.4	ASKAP	Heintz et al. (2020)
	FRB 190714	0.2365	504.13	38.0	ASKAP	Heintz et al. (2020)
	FRB 191001	0.234	507.9	44.7	ASKAP	Heintz et al. (2020)
	FRB 200430	0.16	380.25	27.0	ASKAP	Heintz et al. (2020)
	FRB 201124	0.098	413.52	123.2	ASKAP	Day et al. (2021); Ravi et al. (2021)

3. THE DISTRIBUTIONS OF DM_{IGM} AND DM_{HOST}

The electron number density along different sightlights is not uniform while clustering and fluctuating, so it is difficult to determine the real value of DM_{IGM}. The probability distribution of DM_{IGM} can be modelled by a quasi-Gaussian function with a long tail ([McQuinn 2014](#)). This model includes scatter in the electron distribution, which is mainly caused by random variation of halos along a given sightline. Cosmological simulations indicate that this variation is dominated by galactic feedback redistributing baryons around galactic halos. Strong feedback can expel baryons to larger radii from their host galaxies. This form of DM_{IGM} distribution combines the effect of large-scale structure associated with voids and the sightlines intersecting with clusters. This physical-motivated model of DM_{IGM} distribution provides a successful fit of a wide range of cosmological simulations ([Macquart et al. 2020; Zhang et al. 2021](#)). Using the state-of-the-art IllustrisTNG cosmological simulation ([Springel et al. 2018](#)), [Zhang et al. \(2021\)](#) realistically estimated the distribution of DM_{IGM} at different redshifts ([Zhang et al. 2021](#)). We use the best-fit values of parameters for DM_{IGM} distribution at different redshifts from their paper.

Equation (2) can only describe the average value of DM_{IGM}, while the real value can be fitted by a Gaussian distribution ([McQuinn 2014; Macquart et al. 2020](#)),

$$P_{\text{IGM}}(\Delta) = A\Delta^{-\beta} \exp\left[-\frac{(\Delta^{-\alpha} - C_0)}{2\alpha^2\sigma_{\text{DM}}^2}\right], \Delta > 0, \quad (3)$$

where $\Delta \equiv \text{DM}_{\text{IGM}}/\langle \text{DM}_{\text{IGM}} \rangle$. The indices α and β are related to the inner density profile of gas in halos. [Macquart et al. \(2020\)](#) gave the best fit of $\alpha = 3$ and $\beta = 3$. σ_{DM} is an effective standard deviation. C_0 is a free parameter, which can be fitted when the averaged $\langle \Delta \rangle = 1$. We use the fitting values A , C_0 and σ_{DM} from the state-of-the-art IllustrisTNG simulation ([Zhang et al. 2021](#)).

We use a log-normal distribution to describe the probability distribution of DM_{host}. The distribution is characterized by a median exp μ and width parameter σ_{host} . The distribution of DM_{host} has been derived from the IllustrisTNG cosmological simulation with different properties of galaxies ([Zhang](#)

et al. 2020), such as stellar mass, metallicity and star formation rate. They found that the log-normal distribution provides a successful fit to the galaxy DM distributions. The redshift evolution of $\exp \mu$ and σ_{host} are also given (Zhang et al. 2020).

The distribution of DM_{host} can be well expressed with a log-normal distribution (Macquart et al. 2020; Zhang et al. 2020)

$$P(\text{DM}_{\text{host}}; \mu, \sigma_{\text{host}}) = \frac{1}{\text{DM}_{\text{host}} \sigma_{\text{host}} \sqrt{2\pi}} \exp\left(-\frac{\ln \text{DM}_{\text{host}} - \mu}{2\sigma_{\text{host}}^2}\right), \quad (4)$$

where e^μ and $e^{2\mu+\sigma_{\text{host}}^2}(e^{\sigma_{\text{host}}^2} - 1)$ are the mean and variance of the distribution, respectively. This model has limited theoretical motivation. Interestingly, this model can well describe the DM_{host} distributions derived from state-of-the-art IllustrisTNG simulation (Zhang et al. 2020; Jaroszyński 2020). Zhang et al. (2020) estimated the DM_{host} distribution of repeating FRBs like FRB 121102, repeating FRBs like FRB 180916 and non-repeating FRBs from IllustrisTNG simulation (Zhang et al. 2020). The redshift evolution of DM_{host} is also considered (Zhang et al. 2020). Here we divide the localized FRBs into three types according to host galaxy properties. There are four repeating FRBs in the sample containing 14 localized FRBs, including FRB 121102, FRB 180916, FRB 190711 and FRB 201124A. FRB 190711 is a repeating FRB with a host galaxy of $M_\star = 0.81 \times 10^9 M_\odot$ and $\text{SFR} = 0.42 M_\odot \text{ yr}^{-1}$, which is similar to host galaxy of FRB 121102. FRB 201124A locates in a massive ($\sim 3 \times 10^{10} M_\odot$), star-forming ($\sim \text{afew } M_\odot \text{ yr}^{-1}$) and dusty galaxy, which can be classified into the repeating FRBs like FRB 180916. Obviously, other localized non-repeating FRBs can be classified into non-repeating FRBs.

We estimate the likelihood function by calculating the joint likelihoods of fourteen FRBs

$$\mathcal{L} = \prod_{i=1}^{N_{\text{FRB}}} P_i(\text{DM}'_{\text{FRB},i} | z_i), \quad (5)$$

where $P_i(\text{DM}'_{\text{FRB},i} | z_i)$ is the probability of individual observed FRB with $\text{DM}'_{\text{FRB}} = \text{DM}_{\text{obs}} - \text{DM}_{\text{MW}} = \text{DM}_{\text{host}} + \text{DM}_{\text{IGM}}$. For a FRB at redshift z_i , we have

$$P_i(\text{DM}'_{\text{FRB},i} | z_i) = \int_0^{\text{DM}'_{\text{FRB}}} P_{\text{host}}(\text{DM}_{\text{host}} | \mu, \sigma_{\text{host}}) P_{\text{IGM}}(\text{DM}'_{\text{FRB},i} - \text{DM}_{\text{host}}, z_i) d\text{DM}_{\text{host}}, \quad (6)$$

where $P_{\text{host}}(\text{DM}_{\text{host}} | \mu, \sigma_{\text{host}})$ is the probability density function (PDF) for DM_{host} with a mean value μ and standard deviation σ_{host} , and P_{IGM} is the PDF for DM_{IGM} of FRBs. In the calculation, according to the properties of host galaxy, DM_{host} of FRBs can be divided into repeating FRBs like FRB 121102l, repeating FRBs like FRB 180916 and non-repeating FRBs (Zhang et al. 2020).

4. RESULTS

We use Monte Carlo Markov Chain (MCMC) analysis to estimate H_0 with 14 localized FRBs. The MCMC method is based on Bayesian theory. For any prior distribution, only the properties of the required posterior distribution need to be calculated. Current observations show that there is a general consistency for $\Omega_b h^2$ and Ω_m from different probes. Here we consider a Gaussian distribution of $\Omega_m = 0.315 \pm 0.007$ as the prior distribution of Ω_m (Planck Collaboration et al. 2020). As for $\Omega_b h^2$, it is necessary to apply an independent measurement besides CMB to break the degeneracy between

$\Omega_b h^2$ and H_0 . In the standard theory of Big Bang nucleosynthesis (BBN), the D/H abundance ratio has a strong relationship with the baryonic mass density. We use $\Omega_b h^2 = 0.02235 \pm 0.0049$ derived from the primordial deuterium abundance D/H (Cooke et al. 2018). The tension of H_0 measurements between using Planck data of the CMB and direct model-independent measurements of supernovae in the local universe is obvious. We conservatively assume that the prior distribution of H_0 satisfies a uniform distribution in [0 - 100] km/s/Mpc. The distributions DM_{host} and DM_{IGM} obtained from the IllustrisTNG simulation are used (Zhang et al. 2020, 2021). The steps of MCMC analysis in our method are as follows: (1) The first step is to get the $(z, \text{DM}'_{\text{FRB}})$ parameters of each localized FRBs, where DM'_{FRB} is estimated by subtracting the $\text{DM}_{\text{MW,ISM}}$ value obtained by the NE2001 model and $\text{DM}_{\text{MW,halo}} = 50 \text{ pc cm}^{-3}$ from the observed DM_{obs} value. (2) Equations (3) and (4) are used to model the distributions of DM_{host} and DM_{IGM} with the $(z, \text{DM}'_{\text{FRB}})$ parameters for each localized FRB. (3) From the second step, $\text{DM}'_{\text{FRB}} = \text{DM}_{\text{host}} + \text{DM}_{\text{IGM}}$ is simulated by calculating the convolution of the probability density of DM_{host} and the probability density of DM_{IGM} of each FRB to derive the probability density of DM'_{FRB} . As shown in equation 5, the product of the probability densities of all FRBs is a joint likelihood function. Then MCMC method can be used to fit H_0 , Ω_m and $\Omega_b h^2$. (4) After calculating the total likelihood function, the prior distributions and the initial value of three parameters (H_0 , Ω_m and $\Omega_b h^2$) need to be determined. We assume a uniform prior distribution of H_0 in the interval $[0, 100] \text{ km s}^{-1} \text{ Mpc}^{-1}$, which is a broad scope to show the properties of the posterior distribution. We suppose a initial value of $H_0 = 70 \text{ km s}^{-1} \text{ Mpc}^{-1}$. For Ω_m , we consider 1σ error range $[0.02186, 0.02284]$ given by CMB as a uniform prior distribution. The initial value of Ω_m is consistent with the optimum value of measurement of CMB. Finally, we assume a uniform prior for $\Omega_b h^2$ in the interval $[0.296, 0.32]$, which is consistent with the 1σ range calculated by BBN (Cooke et al. 2018). The initial value of $\Omega_b h^2$ is consistent with the optimum value of BBN measurement. (5) Lastly, we run 1,000 steps of MCMC using the emcee package of Python (Foreman-Mackey et al. 2013) with the likelihood function and the priors. Marginalizing the likelihood functions over the other parameters for ranges restricted by other physical constraints, we derive that the value H_0 measured by fourteen localized FRBs is $64.67^{+5.62}_{-4.66} \text{ km s}^{-1} \text{ Mpc}^{-1}$ with an 8.7% statistical uncertainty, as shown in Figure 2. The H_0 results from Planck CMB data and Cepheid-based distance ladder measurement are also shown in Figure 2. The H_0 value from CMB is well within the 1σ range of that derived from FRBs, while the H_0 value from Cepheid-based distance ladder is out. We also estimate the systematic uncertainty, which is 4.7%. The improvement of measurement accuracy with more localized FRBs will shed light on the Hubble tension.

With the rapid growth of observed number of FRBs, the number of localized FRBs will be greatly improved. Thus, it is necessary to predict how many localized FRBs can give a precise H_0 measurement. Here we predict an optimistic data sample through Monte Carlo simulations and then H_0 can be measured with this optimistic data sample using MCMC analysis, which is the same as that shown in the previous section. Firstly, we suppose that FRBs and long gamma-ray bursts (LGRBs) have similar redshift distribution (Zhou et al. 2014), which is estimated as $f(z) \propto ze^{-z}$ in the redshift $0 < z < 3$. A FRB sample with 100 mock redshifts can be generated from the redshift distribution through Monte Carlo simulations. The DM'_{FRB} corresponding to each mock redshifts can be obtained by Monte Carlo simulation according to its probability distribution function. Then we repeat the MCMC analysis described in the previous section with simulated data. The simulated 100 FRBs give a result of $H_0 = 68.19^{+1.72}_{-1.02} \text{ km s}^{-1} \text{ Mpc}^{-1}$ with an uncertainty of 2.5% at 1σ confidence region as

shown in Figure 3. This precision is comparable to that H_0 measurement with a sample of 75 Milky Way Cepheids (Riess et al. 2021). The result means that 100 localized FRBs can give a high-precision measurement of H_0 , which is obviously exciting and may be realized in the near future. The results of Monte Carlo simulations and MCMC analysis provide an optimistic measurement of H_0 based on the dispersion measure in the $\text{DM}_{\text{IGM}} - z$ relation of localized FRBs.

5. DISCUSSION

The intrinsic properties of FRBs are different (e.g. DM, rotation measure, width). The positng precision will be affected by the sensitivity of the telescope. Considerations of the intrinsic properties of FRB and observational effects contribute to the systematic error that cannot be eliminated. In our study the main error comes from the statistical error due to the small number of the localized FRBs. The larger the amount of data, the smaller the statistical error. In order to mitigate the influence of the statistical error, we consider a sample including all the localized FRBs except FRB 200110E. Once there are enough data, statistical error will not dominate. By that time, it is necessary to select data samples and classify them. According to the four criteria proposed by Macquart et al. (2020), we selected eight FRBs from fifteen localized FRBs. The statistical error is 13.4% applying the same method to constrain H_0 . The main reason for the difference is the relative small sample after selection. We also estimate $\text{DM}_{\text{MW,ISM}}$ based on the YMW16 model (Yao et al. 2017), and find that the result of H_0 is similar as that of NE2001 model. So the choice of electron density model of Milky Way does not affect the final result.

An annoying but unavoidable problem is systematic uncertainty, which includes all the errors except statistical error. It cannot be eliminated while statistical error can be eliminated with more data. Therefore, it is necessary to consider the influence of systematic error in our study. The systematic error of FRB dispersion measure observation is very small, which can be ignored compared with other systematic error. However, the systematic error caused by the positioning error of FRB can not be ignored, so more accurate positioning is necessary. Moreover, there will be observation selection effect between different telescopes and different FRB, which is one of the components of the systematic error.

The systematic uncertainty caused by the choice of the prior of $\Omega_b h^2$ and Ω_m also needs to be considered. Since the uncertainty of $\Omega_b h^2$ is about 2% from BBN, we chose the systematic uncertainty as 2%. Similarly, the uncertainty of Ω_m is about 4%, we suppose the value of the systematic uncertainty as 4%. The calculation of systematic error satisfies the error transfer formula. According to equation (2), the systematic error of H_0 mainly comes from the systematic error of $\Omega_b h^2$ and Ω_m . We estimate that the systematic error of H_0 is about 4.7%, which is smaller than the statistical error of 8%. However, the influence of systematic error does not have a rule and can not be eliminated. More precise measurements of $\Omega_b h^2$ and Ω_m are needed.

In general, the result of considering the different distribution of DM_{host} and DM_{IGM} to constrain the Hubble constant is optimistic, which shows that FRB can be a reliable cosmological probe. With more localized FRBs and more precise measurements of $\Omega_b h^2$ and Ω_m , we can better constrain the Hubble constant to provide a new direction for solving the “Hubble tension”.

ACKNOWLEDGEMENTS

This work was supported by the National Natural Science Foundation of China (grant No. U1831207) and the Fundamental Research Funds for the Central Universities (No. 0201-14380045). We thank Z. G. Dai, Z. H. Fan and Z.Q.H for helpful discussion.

REFERENCES

Abbott, B. P., Abbott, R., Abbott, T. D., et al. 2017, *Nature*, 551, 85, doi: [10.1038/nature24471](https://doi.org/10.1038/nature24471)

Bannister, K. W., Deller, A. T., Phillips, C., et al. 2019, *Science*, 365, 565, doi: [10.1126/science.aaw5903](https://doi.org/10.1126/science.aaw5903)

Bhandari, S., & Flynn, C. 2021, *Universe*, 7, 85, doi: [10.3390/universe7040085](https://doi.org/10.3390/universe7040085)

Bhandari, S., Sadler, E. M., Prochaska, J. X., et al. 2020, *ApJL*, 895, L37, doi: [10.3847/2041-8213/ab672e](https://doi.org/10.3847/2041-8213/ab672e)

Bhardwaj, M., Gaensler, B. M., Kaspi, V. M., et al. 2021, *ApJL*, 910, L18, doi: [10.3847/2041-8213/abeaa6](https://doi.org/10.3847/2041-8213/abeaa6)

Chatterjee, S., Law, C. J., Wharton, R. S., et al. 2017, *Nature*, 541, 58, doi: [10.1038/nature20797](https://doi.org/10.1038/nature20797)

Chime/Frb Collaboration, Amiri, M., Andersen, B. C., et al. 2020, *Nature*, 582, 351, doi: [10.1038/s41586-020-2398-2](https://doi.org/10.1038/s41586-020-2398-2)

Chittidi, J. S., Simha, S., Mannings, A., et al. 2020, arXiv e-prints, arXiv:2005.13158. <https://arxiv.org/abs/2005.13158>

Cooke, R. J., Pettini, M., & Steidel, C. C. 2018, *ApJ*, 855, 102, doi: [10.3847/1538-4357/aaab53](https://doi.org/10.3847/1538-4357/aaab53)

Cordes, J. M., & Chatterjee, S. 2019, *ARA&A*, 57, 417, doi: [10.1146/annurev-astro-091918-104501](https://doi.org/10.1146/annurev-astro-091918-104501)

Cordes, J. M., & Lazio, T. J. W. 2002, arXiv e-prints, astro. <https://arxiv.org/abs/astro-ph/0207156>

Cuceu, A., Farr, J., Lemos, P., & Font-Ribera, A. 2019, *JCAP*, 2019, 044, doi: [10.1088/1475-7516/2019/10/044](https://doi.org/10.1088/1475-7516/2019/10/044)

Day, C. K., Bhandari, S., Deller, A. T., Shannon, R. M., & Moss, V. A. 2021, *The Astronomer's Telegram*, 14515, 1

Deng, W., & Zhang, B. 2014, *ApJL*, 783, L35, doi: [10.1088/2041-8205/783/2/L35](https://doi.org/10.1088/2041-8205/783/2/L35)

Di Valentino, E., Mena, O., Pan, S., et al. 2021, arXiv e-prints, arXiv:2103.01183. <https://arxiv.org/abs/2103.01183>

Foreman-Mackey, D., Conley, A., Meierjurgen, Farr, W., et al. 2013, emcee: The MCMC Hammer. <http://ascl.net/1303.002>

Freedman, W. L. 2017, *Nature Astronomy*, 1, 0169, doi: [10.1038/s41550-017-0169](https://doi.org/10.1038/s41550-017-0169)

Gao, H., Li, Z., & Zhang, B. 2014, *ApJ*, 788, 189, doi: [10.1088/0004-637X/788/2/189](https://doi.org/10.1088/0004-637X/788/2/189)

Hagstotz, S., Reischke, R., & Lilow, R. 2021, arXiv e-prints, arXiv:2104.04538. <https://arxiv.org/abs/2104.04538>

Heintz, K. E., Prochaska, J. X., Simha, S., et al. 2020, *ApJ*, 903, 152, doi: [10.3847/1538-4357/abb6fb](https://doi.org/10.3847/1538-4357/abb6fb)

Inoue, S. 2004, *MNRAS*, 348, 999, doi: [10.1111/j.1365-2966.2004.07359.x](https://doi.org/10.1111/j.1365-2966.2004.07359.x)

Ioka, K. 2003, *ApJL*, 598, L79, doi: [10.1086/380598](https://doi.org/10.1086/380598)

Jaroszynski, M. 2019, *MNRAS*, 484, 1637, doi: [10.1093/mnras/sty3529](https://doi.org/10.1093/mnras/sty3529)

Jaroszyński, M. 2020, *AcA*, 70, 87, doi: [10.32023/0001-5237/70.2.1](https://doi.org/10.32023/0001-5237/70.2.1)

Katz, J. I. 2018, *Progress in Particle and Nuclear Physics*, 103, 1, doi: [10.1016/j.ppnp.2018.07.001](https://doi.org/10.1016/j.ppnp.2018.07.001)

Kirsten, F., Marcote, B., Nimmo, K., et al. 2021, arXiv e-prints, arXiv:2105.11445. <https://arxiv.org/abs/2105.11445>

Law, C. J., Butler, B. J., Prochaska, J. X., et al. 2020, *ApJ*, 899, 161, doi: [10.3847/1538-4357/aba4ac](https://doi.org/10.3847/1538-4357/aba4ac)

Li, Z.-X., Gao, H., Ding, X.-H., Wang, G.-J., & Zhang, B. 2018, *Nature Communications*, 9, 3833, doi: [10.1038/s41467-018-06303-0](https://doi.org/10.1038/s41467-018-06303-0)

Lorimer, D. R., Bailes, M., McLaughlin, M. A., Narkevic, D. J., & Crawford, F. 2007, *Science*, 318, 777, doi: [10.1126/science.1147532](https://doi.org/10.1126/science.1147532)

Macquart, J. P., Prochaska, J. X., McQuinn, M., et al. 2020, *Nature*, 581, 391, doi: [10.1038/s41586-020-2300-2](https://doi.org/10.1038/s41586-020-2300-2)

Marcote, B., Nimmo, K., Hessels, J. W. T., et al. 2020, *Nature*, 577, 190, doi: [10.1038/s41586-019-1866-z](https://doi.org/10.1038/s41586-019-1866-z)

McQuinn, M. 2014, *ApJL*, 780, L33, doi: [10.1088/2041-8205/780/2/L33](https://doi.org/10.1088/2041-8205/780/2/L33)

Muñoz, J. B., Kovetz, E. D., Dai, L., & Kamionkowski, M. 2016, *PhRvL*, 117, 091301, doi: [10.1103/PhysRevLett.117.091301](https://doi.org/10.1103/PhysRevLett.117.091301)

Petroff, E., Hessels, J. W. T., & Lorimer, D. R. 2019, A&A Rv, 27, 4, doi: [10.1007/s00159-019-0116-6](https://doi.org/10.1007/s00159-019-0116-6)

Planck Collaboration, Aghanim, N., Akrami, Y., et al. 2020, A&A, 641, A6, doi: [10.1051/0004-6361/201833910](https://doi.org/10.1051/0004-6361/201833910)

Platts, E., Weltman, A., Walters, A., et al. 2019, PhR, 821, 1, doi: [10.1016/j.physrep.2019.06.003](https://doi.org/10.1016/j.physrep.2019.06.003)

Prochaska, J. X., & Zheng, Y. 2019, MNRAS, 485, 648, doi: [10.1093/mnras/stz261](https://doi.org/10.1093/mnras/stz261)

Prochaska, J. X., Macquart, J.-P., McQuinn, M., et al. 2019, Science, 366, 231, doi: [10.1126/science.aay0073](https://doi.org/10.1126/science.aay0073)

Rajwade, K. M., Mickaliger, M. B., Stappers, B. W., et al. 2020, MNRAS, 495, 3551, doi: [10.1093/mnras/staa1237](https://doi.org/10.1093/mnras/staa1237)

Ravi, V., Catha, M., D'Addario, L., et al. 2019, Nature, 572, 352, doi: [10.1038/s41586-019-1389-7](https://doi.org/10.1038/s41586-019-1389-7)

Ravi, V., Law, C. J., Li, D., et al. 2021, arXiv e-prints, arXiv:2106.09710. <https://arxiv.org/abs/2106.09710>

Riess, A. G. 2020, Nature Reviews Physics, 2, 10, doi: [10.1038/s42254-019-0137-0](https://doi.org/10.1038/s42254-019-0137-0)

Riess, A. G., Casertano, S., Yuan, W., et al. 2021, ApJL, 908, L6, doi: [10.3847/2041-8213/abdbaf](https://doi.org/10.3847/2041-8213/abdbaf)

Shull, J. M., Smith, B. D., & Danforth, C. W. 2012, ApJ, 759, 23, doi: [10.1088/0004-637X/759/1/23](https://doi.org/10.1088/0004-637X/759/1/23)

Springel, V., Pakmor, R., Pillepich, A., et al. 2018, MNRAS, 475, 676, doi: [10.1093/mnras/stx3304](https://doi.org/10.1093/mnras/stx3304)

The CHIME/FRB Collaboration, Andersen, B. C., Bandura, K., et al. 2021a, arXiv e-prints, arXiv:2107.08463. <https://arxiv.org/abs/2107.08463>

The CHIME/FRB Collaboration, ;, Amiri, M., et al. 2021b, arXiv e-prints, arXiv:2106.04352. <https://arxiv.org/abs/2106.04352>

Walters, A., Weltman, A., Gaensler, B. M., Ma, Y.-Z., & Witzemann, A. 2018, ApJ, 856, 65, doi: [10.3847/1538-4357/aaaf6b](https://doi.org/10.3847/1538-4357/aaaf6b)

Wang, Y. K., & Wang, F. Y. 2018, A&A, 614, A50, doi: [10.1051/0004-6361/201731160](https://doi.org/10.1051/0004-6361/201731160)

Xiao, D., Wang, F., & Dai, Z. 2021, Science China Physics, Mechanics, and Astronomy, 64, 249501, doi: [10.1007/s11433-020-1661-7](https://doi.org/10.1007/s11433-020-1661-7)

Yao, J. M., Manchester, R. N., & Wang, N. 2017, ApJ, 835, 29, doi: [10.3847/1538-4357/835/1/29](https://doi.org/10.3847/1538-4357/835/1/29)

Yu, H., & Wang, F. Y. 2017, A&A, 606, A3, doi: [10.1051/0004-6361/201731607](https://doi.org/10.1051/0004-6361/201731607)

Zhang, G. Q., Yu, H., He, J. H., & Wang, F. Y. 2020, ApJ, 900, 170, doi: [10.3847/1538-4357/abaa4a](https://doi.org/10.3847/1538-4357/abaa4a)

Zhang, Z. J., Yan, K., Li, C. M., Zhang, G. Q., & Wang, F. Y. 2021, ApJ, 906, 49, doi: [10.3847/1538-4357/abceb9](https://doi.org/10.3847/1538-4357/abceb9)

Zheng, Z., Ofek, E. O., Kulkarni, S. R., Neill, J. D., & Juric, M. 2014, ApJ, 797, 71, doi: [10.1088/0004-637X/797/1/71](https://doi.org/10.1088/0004-637X/797/1/71)

Zhou, B., Li, X., Wang, T., Fan, Y.-Z., & Wei, D.-M. 2014, PhRvD, 89, 107303, doi: [10.1103/PhysRevD.89.107303](https://doi.org/10.1103/PhysRevD.89.107303)

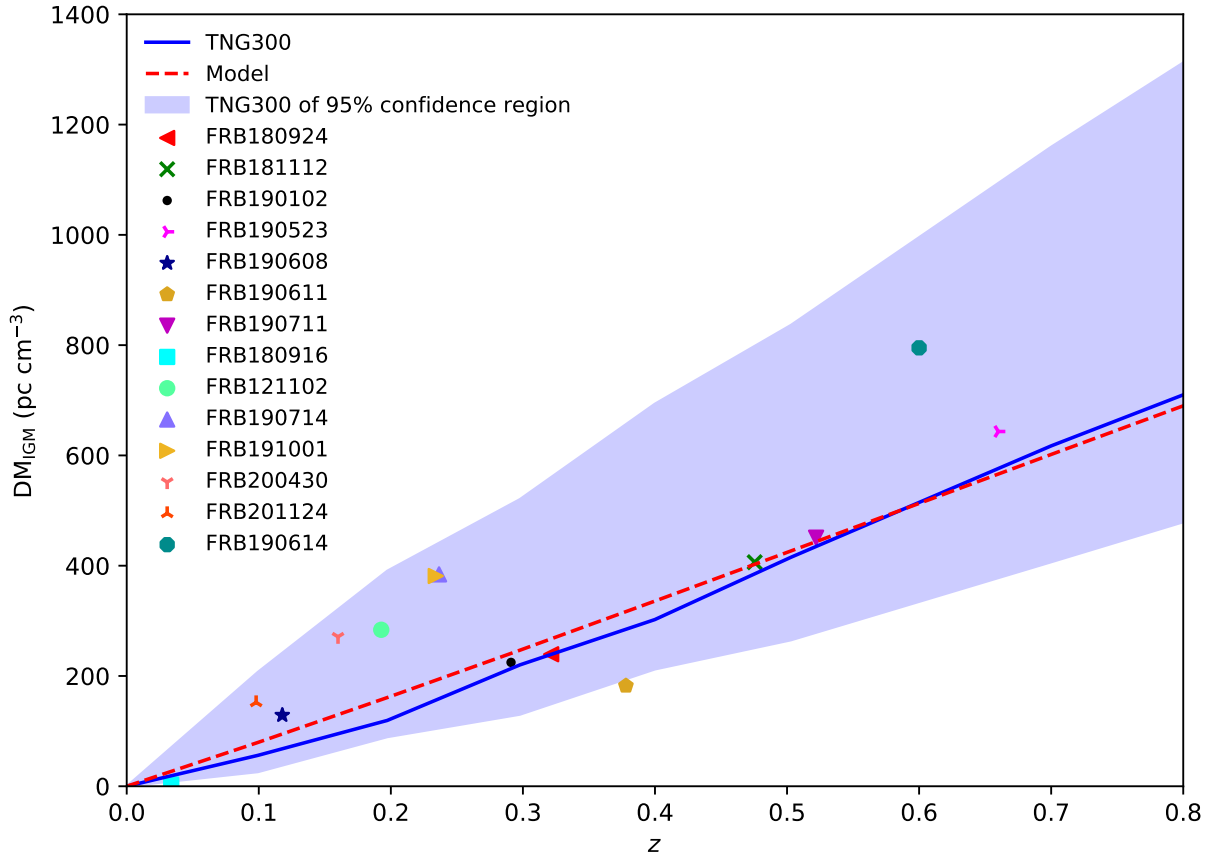


Figure 1. The DM_{IGM} - z relation for fourteen localized FRBs. The scattered points are the DM_{IGM} values of the 14 localized FRBs. The DM_{IGM} values are derived by correcting the observed dispersion measure DM_{obs} for the estimated contributions from our Galaxy and the FRB host galaxy. The $DM_{MW,ISM}$ is deduced from NE2001 model, and $DM_{MW,halo}$ is adopted as 50 pc cm^{-3} . We use the median value of DM_{host} at different redshifts from IllustrisTNG 300 cosmological simulation (Zhang et al. 2020). The red dotted line shows model of equation (2) with $\Omega_m = 0.315$, $\Omega_B h^2 = 0.02235$ and $H_0 = 70 \text{ km s}^{-1} \text{ Mpc}^{-1}$. The blue line corresponds to the DM_{IGM} result from the IllustrisTNG 300 cosmological simulation and the purple shaded area is the 95% confidence region (Zhang et al. 2021). Apparently, some FRBs significantly deviates from the averaged DM_{IGM} by considering the median value of DM_{host} . Therefore, in order to obtain reliable cosmological constraints, the probability distributions of DM_{IGM} and DM_{host} must be considered.

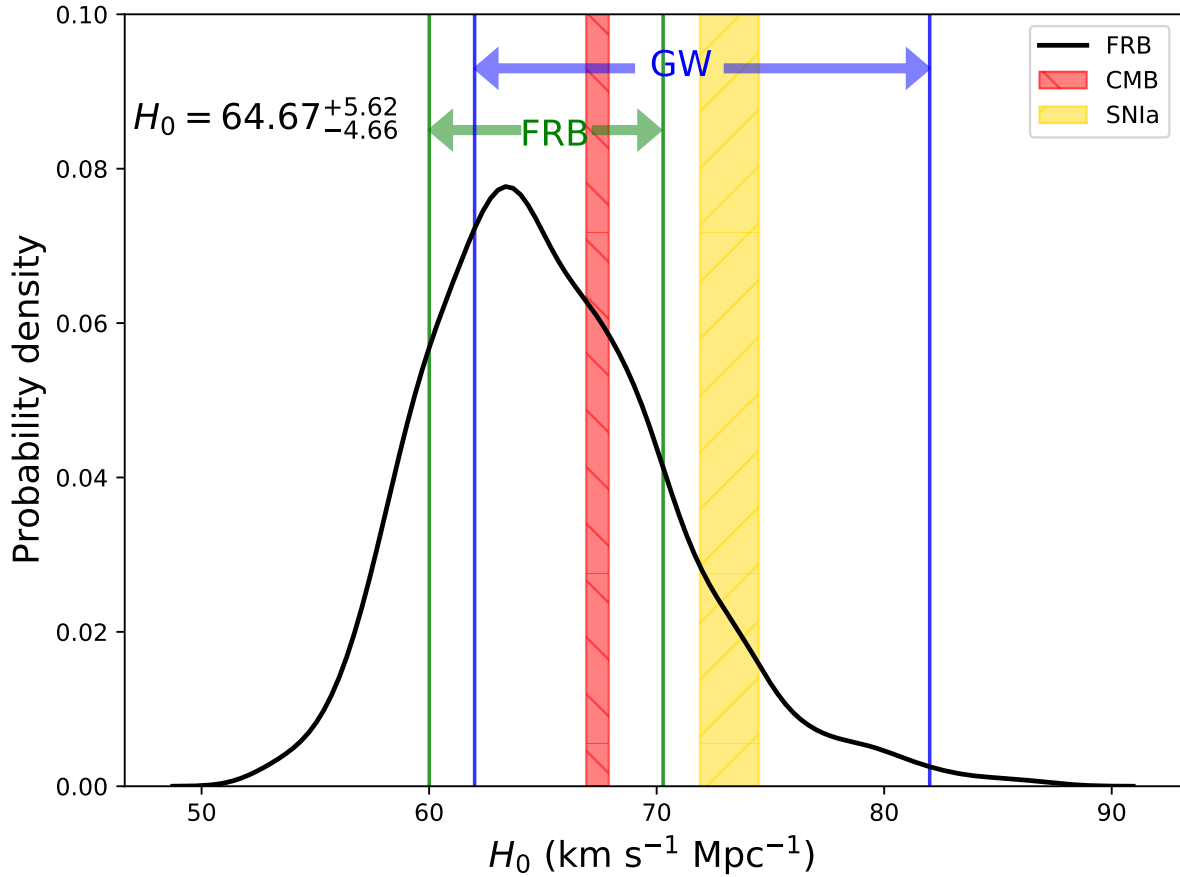


Figure 2. The probability density distribution of H_0 from 14 localized FRBs. The black solid line shows the probability density distribution of H_0 . While the area between the two green vertical line shows the result $H_0 = 64.67^{+5.62}_{-4.66} \text{ km s}^{-1} \text{ Mpc}^{-1}$ with 1σ uncertainty. The blue vertical lines corresponds to the H_0 value derived by GW170817 (Abbott et al. 2017). The coral and yellow regions correspond to the 1σ uncertainty range of H_0 reported by SH0ES (Riess et al. 2021) and Planck (Planck Collaboration et al. 2020), respectively.

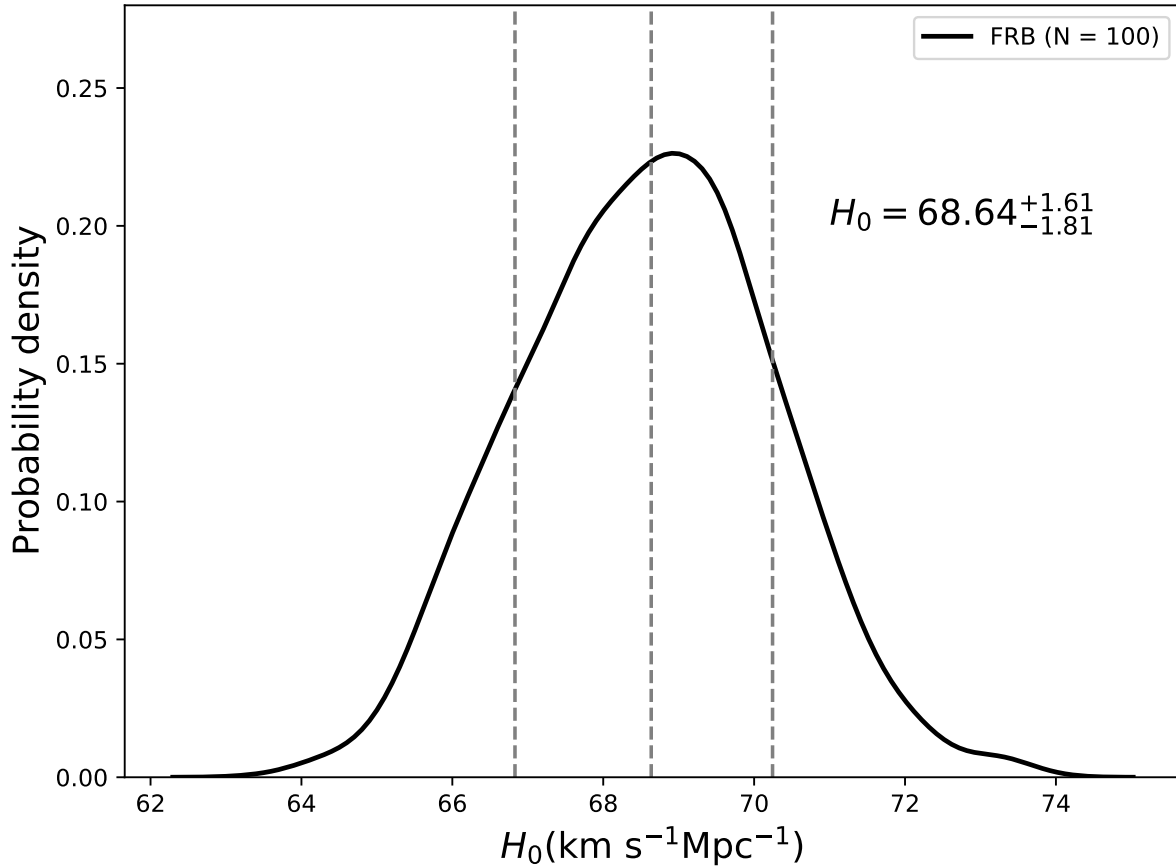


Figure 3. The probability density distribution of H_0 from 100 simulated FRBs. The black solid line corresponding to the probability density distribution of H_0 from 100 simulated FRBs. The dotted line in the middle corresponds to the median value of the distribution, and the dotted lines on both sides represent the 1σ confidence interval. The result is $H_0 = 68.64^{+1.61}_{-1.81} \text{ km s}^{-1} \text{ Mpc}^{-1}$ with 1σ error. The statistical error is about 2.6%.